Journal of Neuroscience Methods 251 (2015) 37–46

Contents lists available at ScienceDirect

Journal of Neuroscience Methods

journal homepage: www.elsevier.com/locate/jneumeth

Computational Neuroscience

Detection of K-complexes and sleep spindles (DETOKS) using sparse optimization

Ankit Parekh[a,*], Ivan W. Selesnick[b], David M. Rapoport[c], Indu Ayappa[c]

[a] Department of Mathematics, School of Engineering, New York University, USA
[b] Department of Electrical and Computer Engineering, School of Engineering, New York University, USA
[c] Department of Medicine, Division of Pulmonary, Critical Care and Sleep Medicine, School of Medicine, New York University, USA

HIGHLIGHTS

- Proposed method outperforms six widely used automated detectors for sleep spindles and K-complexes.
- Proposed method is based on a three-component EEG time-series model.
- Average F1 score for sleep spindle detection are 0.70 ± 0.03 and for K-complex detection are 0.57 ± 0.02.

ARTICLE INFO

Article history:
Received 8 March 2015
Received in revised form 3 April 2015
Accepted 7 April 2015
Available online 6 May 2015

Keywords:
Sparse signal
Convex optimization
Sleep spindle detection
K-complex detection

ABSTRACT

Background: This paper addresses the problem of detecting sleep spindles and K-complexes in human sleep EEG. Sleep spindles and K-complexes aid in classifying stage 2 NREM human sleep.
New method: We propose a non-linear model for the EEG, consisting of a transient, low-frequency, and an oscillatory component. The transient component captures the non-oscillatory transients in the EEG. The oscillatory component admits a sparse time–frequency representation. Using a convex objective function, this paper presents a fast non-linear optimization algorithm to estimate the components in the proposed signal model. The low-frequency and oscillatory components are used to detect K-complexes and sleep spindles respectively.
Results and comparison with other methods: The performance of the proposed method is evaluated using an online EEG database. The F1 scores for the spindle detection averaged 0.70 ± 0.03 and the F1 scores for the K-complex detection averaged 0.57 ± 0.02. The Matthews Correlation Coefficient and Cohen's Kappa values were in a range similar to the F1 scores for both the sleep spindle and K-complex detection. The F1 scores for the proposed method are higher than existing detection algorithms.
Conclusions: Comparable run-times and better detection results than traditional detection algorithms suggests that the proposed method is promising for the practical detection of sleep spindles and K-complexes.

1. Introduction

Sleep spindles comprise of a group of rhythmic waves that progressively increase and decrease in amplitude (Silber et al., 2007). They are of at least 0.5 s in duration and have frequencies in the range of 12–14 Hz (Berry et al., 2013). Recent studies have suggested an extended frequency range from 11 Hz to 16 Hz (Devuyst et al., 2006; Warby et al., 2014). Sleep spindles are believed to play an important role in synaptic plasticity and memory consolidation during sleep (Fogel and Smith, 2011). Alteration in the density of sleep spindles is observed in patients with disorders such as schizophrenia (Ferrarelli et al., 2007; Wamsley et al., 2012), autism (Limoges et al., 2005) and other neurodegenerative and sleep disorders (Petit et al., 2004). This leads to mounting belief that sleep spindles may be valuable as diagnostic biomarkers (Warby et al., 2014).

The K-complex is a transient waveform with a biphasic morphology, characterized by a negative sharp wave followed by a positive one (Richard and Lengelle, 1998). The K-complex is a relatively large waveform having a duration between 0.5 and 1.5 s with an amplitude larger than 75 μV.

The detection of sleep spindles and K-complexes aid in the scoring of stage N2 of NREM sleep. Traditionally, these morphologically

* Corresponding author at: 6 Metrotech Center, Jay St., Brooklyn, NY, USA. Tel.: +1 7182603666.
E-mail address: ankit.parekh@nyu.edu (A. Parekh).

http://dx.doi.org/10.1016/j.jneumeth.2015.04.006
0165-0270/

distinct waveforms have been identified manually by trained experts in sleep clinics. This is subjective, time consuming, and prone to errors. The low and widely varying inter-rater agreement for sleep spindle and K-complex detection adds to the complexity of the overall scoring process and diagnostic utility. The Cohen's κ coefficient for inter-rater manual scoring ranges from 0.46 to 0.89 (Stepnowsky et al., 2013). Some studies have reported an even lower κ coefficient (Devuyst et al., 2010, 2011). Solving the above issues require a reliable automated detector for sleep spindles and K-complexes.

1.1. Detection algorithms

Numerous automated detectors have been developed over the past few years for detecting sleep spindles and K-complexes. At the core of many of the spindle detection algorithms is the use of a constant or adaptive threshold after bandpass filtering the input EEG (Wamsley et al., 2012; Wendt et al., 2012; Martin et al., 2013; Gais et al., 2002). Few detectors have been designed to simultaneously detect spindles and K-complexes, whereas most are designed to detect one or the other (Camilleri et al., 2014). The bandpass filter used is also excited by transients present in the input EEG. Much of the effort of these algorithms is to either pre-process (Jaleel et al., 2014), or post-process (Motamedi-Fakhr et al., 2014) the bandpass filtered data, so as to distinguish spindles from transients.

To reduce this overhead, algorithms have been designed using neural networks (Gorur et al., 2002), sleep spindle morphology (Costa et al., 2012), support vector machines (Acir and Güzeli, 2005), time–frequency methods via the short-time Fourier transform (STFT) (Devuyst et al., 2011; Motamedi-Fakhr et al., 2014) and adaptive time–frequency methods (Durka and Blinowska, 1996; Durka et al., 2001). The drawback of using machine learning methods is that they may suffer from over-learning. This increases the number of falsely detected spindles, as compared to scoring by experts (based on the specificity values) (Gorur et al., 2002). A non-linear pre-processor for the EEG using convex optimization was shown to successfully separate the transients from the spindle activity (Parekh et al., 2014). However, that approach is computationally inefficient as it utilizes two STFT's with high overlap between consecutive windows.

The Teager–Kaiser energy operator (TKEO) has been used for the automatic detection of K-complexes, in conjunction with the time–frequency and neural network methods highlighted above (Erdamar et al., 2012; Richard and Lengelle, 1998; Strungaru and Popescu, 1998). The TKEO is helpful in extracting the sharp rising and falling edges of the K-complex. However, the presence of transients adversely affects the performance of these algorithms as the TKEO is not able to successfully extract the K-complex activity in the input EEG signal. The spindle and K-complex activity can be made more prominent by suppressing transients in the EEG. However, this suppression is difficult using linear filters, thereby motivating non-linear methods (Selesnick, 2011).

1.2. Contribution

In this paper we propose a non-linear method for the detection of sleep spindles and K-complexes (DETOKS). We model the input EEG as a sum of three components:

1) Transient. The transient component is modeled as a sparse signal possessing a sparse first-order derivative. Essentially, the transient component is comprised of spikes on a baseline of zero.
2) Low-frequency. The low-frequency component of the EEG signal.
3) Oscillations. The rhythmic oscillations in the EEG signal that admit a sparse time–frequency representation.

To estimate the three components from the input EEG signal, we propose an optimization problem utilizing a convex objective function and also derive a fast algorithm for its solution. Post estimation of the components, we use the low-frequency and the oscillatory components for the detection of K-complexes and sleep spindles respectively. Since the proposed method separates the transients from the low-frequency and oscillatory components used for detection, the bandpass filter reveals the spindle activity much more prominently with respect to the baseline. Thus, the proposed approach can make traditional spindle detection methods robust by prefacing them with non-linear transient removal.

We list the preliminaries in Section 2 and formulate the DETOKS problem in Section 3. We illustrate the suppression of the transients in the input EEG with various examples in Section 4. We evaluate the performance of DETOKS by applying it on an online EEG database in Section 5. Specifically, we compare spindle and K-complex detection results using the proposed DETOKS method and existing automated detectors by (Wendt et al., 2012; Martin et al., 2013; Wamsley et al., 2012; Bódizs et al., 2009; Gais et al., 2002; Devuyst et al., 2011, 2010).

2. Preliminaries

2.1. Notation

We denote vectors and matrices by lower and upper case letters respectively. The N-point signal y is represented by the vector

$$\mathrm{y} = [y(0), \ldots, y(N-1)]^T, \qquad \mathrm{y} \in \mathbb{R}^N, \tag{1}$$

where $[\cdot]^T$ represents the transpose. The ℓ_1 and ℓ_2 norm of the vector y are defined as

$$\|\mathrm{y}\|_1 := \sum_n |y(n)|, \quad \|\mathrm{y}\|_2 := \left(\sum_n |y(n)|^2\right)^{1/2}. \tag{2}$$

The matrix D is defined as

$$\mathrm{D} := \begin{bmatrix} -1 & 1 & & & \\ & -1 & 1 & & \\ & & \ddots & \ddots & \\ & & & -1 & 1 \end{bmatrix}. \tag{3}$$

Using the matrix D, the first order difference of an N-point discrete signal x is given by Dx. Here D is of size $(N-1)\times N$. The soft-threshold function (Donoho, 1995) for $\lambda > 0$, $\lambda \in \mathbb{R}$ is defined as

$$\mathrm{soft}(x, \lambda) := \begin{cases} x - \lambda \dfrac{x}{|x|}, & |x| > \lambda \\ 0, & |x| \le \lambda, \end{cases} \qquad x \in \mathbb{C}. \tag{4}$$

The soft-threshold function as defined in (4) is valid for complex valued x. The notation soft(x, λ) implies that the soft-threshold function is applied element-wise to x with a threshold of λ. The Teager–Kaiser Energy Operator (TKEO), $T(\cdot)$, for a discrete-time signal y is defined as

$$[T(\mathrm{y})]_n := y^2(n) - y(n-1)\cdot y(n+1). \tag{5}$$

2.2. Sparse optimization

To estimate a signal x, possessing a sparse or approximately sparse derivative, from a noisy mixture

$$\mathrm{y} = \mathrm{x} + \mathrm{w}, \tag{6}$$

it is common to minimize the ℓ_1 norm of the first-order difference Dx subject to a data fidelity constraint (Rudin et al., 1992). Thus, a suitable optimization problem for estimating x is

$$\hat{x} = \underset{x}{\operatorname{argmin}} \left\{ \frac{1}{2}\|y - x\|_2^2 + \lambda \|Dx\|_1 \right\}. \tag{7}$$

The value $\lambda > 0$ controls the sparsity of the derivative of x, where the ℓ_1 norm is used as a convex proxy for sparsity. The problem in (7) is known as total variation denoising (TVD) whose solution in linear time is given in (Condat, 2013). If x is also sparse, i.e., it comprises of spikes on a baseline of zero, then an appropriate optimization problem is given by

$$\hat{x} = \underset{x}{\operatorname{argmin}} \left\{ \frac{1}{2}\|y - x\|_2^2 + \lambda_1 \|x\|_1 + \lambda_2 \|Dx\|_1 \right\}. \tag{8}$$

This problem is known as the fused lasso (Rinaldo, 2009; Tibshirani et al., 1369) and its solution is given by

$$x = \text{soft}(\text{tvd}(y, \lambda_2), \lambda_1), \tag{9}$$

where $\text{tvd}(\cdot, \cdot)$ represents the solution to the TV denoising problem (7).

2.3. Short-time Fourier Transform

Signals that admit a sparse representation can be described by a small number of coefficients using an appropriate transform. Such representations, when they exist, can account for most of the energy contained in a signal (Mallat, 2009). Recently over-complete transforms have been exploited for the sparse representation of signals (Chen et al., 1998). A signal consisting of oscillatory pulses can be represented sparsely using the STFT. The STFT requires specification of several parameters such as window length, overlapping factor, and the discrete Fourier transform (DFT) length.

In this work, we use a window length of 1.28 s for the STFT and a DFT length equal to the window length. This choice of window length ensures that the DFT length is a power of 2 when the sampling frequency is 50 Hz, 100 Hz, or 200 Hz. In case the EEG is sampled at 128 Hz, we use a one-second window. We use 75% overlapping between windows, i.e., a hop size of one quarter of the window length. Hence, the STFT is 4-times over-sampled.

Precisely, using a time–frequency array for STFT coefficients of size $M \times K$, for a signal y of length N, we define $\Phi : \mathbb{C}^{M\times K} \mapsto \mathbb{C}^N$ as

$$\Phi c := \text{STFT}^{-1}(c), \tag{10}$$

and $\Phi^H : \mathbb{C}^N \mapsto \mathbb{C}^{M\times K}$ is defined as

$$\Phi^H y := \mathit{STFT}(y). \tag{11}$$

Using a sine window, we implement the STFT to have the perfect reconstruction property, specifically

$$\Phi\Phi^H = I, \tag{12}$$

where Φ^H represents the Hermitian transpose of Φ (Selesnick, 2015).

3. Simultaneous detection using DETOKS

3.1. Problem formulation

We model the EEG signal as

$$y = f + x + s + w, \qquad f, x, s, w \in \mathbb{R}^N, \tag{13}$$

where f represents a low-frequency signal, x is a sparse signal with sparse first-order derivative, s consists of rhythmic oscillations and is sparse with respect to Φ, and w represents the residual. This kind of a signal model is similar to the one used for transient removal and suppression in (Selesnick et al., 2014; Parekh et al., 2014). In contrast to (Parekh et al., 2014), we model the sparse transient component using a sparse first-order derivative rather than an STFT.

We seek estimates for the components x, f and s from the given signal y in (13). The component s can be modeled as

$$s = \Phi c, \tag{14}$$

where $c \in \mathbb{C}^{M\times K}$ is the STFT coefficient array. Using a lowpass filter L we define the highpass filter H as

$$H := I - L, \tag{15}$$

assuming that the frequency response of the lowpass filter is zero-phase or at least approximately zero-phase (Selesnick et al., 2014). For a highpass filter having a $2d$−order zero at $z = 1$, the matrix H is of size $(N - 2d) \times N$ when applied to a signal of length N. Applying the highpass filter to the signal model in (13), we have

$$H(y - x - \Phi c) \approx w. \tag{16}$$

In order to estimate the components x and c from a given y and minimize the energy of the residual w, we propose the following unconstrained optimization problem,

$$\underset{x,c}{\operatorname{argmin}} \left\{ \frac{1}{2}\|H(y - x - \Phi c)\|_2^2 + \lambda_0 \|x\|_1 + \lambda_1 \|Dx\|_1 + \lambda_2 \|c\|_1 \right\}. \tag{17}$$

The objective function in (17) promotes the sparsity of the signal x, its first-order derivative Dx, and the STFT coefficient array c, using the ℓ_1 norm. The scalars λ_0, λ_1 and λ_2 are regularization parameters. We set the highpass filter H to be a zero-phase recursive discrete-time filter, that we write as

$$H = A^{-1}B, \tag{18}$$

where A and B are banded[1] Toeplitz matrices, as described in Section VI of (Selesnick et al., 2014). Note that A is of size $(N - 2d) \times (N - 2d)$ and B is of size $(N - 2d) \times N$, when the $2d$−order highpass filter is applied to a signal of length N. The banded structure of A and B aids in the computational efficiency of the algorithm that will be developed in the next sub-section.

3.2. Algorithm

Various problems arising in signal processing and bio-medical engineering are formulated as convex optimization problems. The objective function in (17) is also convex, and can be minimized via convex optimization algorithms. There exists a wealth of algorithms for solving problems of type (17) with two or more sparsity inducing penalties (Chambolle and Pock, 2011; Combettes and Pesquet, 2007). In particular, we apply Douglas-Rachford splitting (Combettes and Pesquet, 2011) to solve (17). The Douglas-Rachford splitting approach results in the well-known alternating direction method of multipliers (ADMM) (Afonso et al., 2010; Gabay, 1983). Applying variable splitting, we rewrite (17) as

$$\underset{u_1,u_2,x,c}{\arg\min} \left\{ \frac{1}{2}\|H(y - u_1 - \Phi u_2)\|_2^2 + \lambda_0 \|x\|_1 + \lambda_1 \|Dx\|_1 + \lambda_2 \|c\|_1 \right\} \tag{19a}$$

$$\text{s.t.} \quad u_1 = x, \qquad u_2 = c. \tag{19b}$$

[1] A banded matrix is a type of sparse matrix, whose non-zero entries are restricted on the main diagonal and one or more diagonals on either side of the main diagonal.

Note that (19) is equivalent to (17). Using the scaled augmented Lagrangian (Boyd et al., 2010), we can minimize (19) by the following iterative procedure.

Repeat :

$$u_1, u_2 \leftarrow \underset{u_1,u_2}{arg\,min} \left\{ \frac{1}{2}\|H(y - u_1 - \Phi u_2)\|_2^2 + \frac{\mu}{2}\|u_1 - x - d_1\|_2 + \frac{\mu}{2}\|u_2 - c - d_2\|_2^2 \right\} \tag{20a}$$

$$x, c \leftarrow \underset{x,c}{arg\,min} \left\{ \lambda_0\|x\|_1 + \lambda_1\|Dx\|_1 + \lambda_2\|c\|_1 + \frac{\mu}{2}\|u_1 - x - d_1\|_2 + \frac{\mu}{2}\|u_2 - c - d_2\|_2^2 \right\} \tag{20b}$$

$$d_1 \leftarrow d_1 - (u_1 - x) \tag{20c}$$

$$d_2 \leftarrow d_2 - (u_2 - c) \tag{20d}$$

where $\mu > 0$. The minimization in (20b) is separable, thus x and c can be minimized independently. Thus, we can write (20b) as

$$x \leftarrow \underset{x}{arg\,min} \left\{ \lambda_0\|x\|_1 + \lambda_1\|Dx\|_1 + \frac{\mu}{2}\|u_1 - x - d_1\|_2 \right\} \tag{21a}$$

$$c \leftarrow \underset{c}{arg\,min} \left\{ \lambda_2\|c\|_1 + \frac{\mu}{2}\|u_2 - c - d_2\|_2^2 \right\} \tag{21b}$$

The solutions to (21a) and (21b) are readily implemented using the solution to the fused lasso problem as described in Section 2.2 and the soft threshold function (4). Specifically, the solutions to (21a) and (21b) are given by

$$x \leftarrow \text{soft}(\text{tvd}(u_1 - d_1, \lambda_1/\mu), \lambda_0/\mu), \tag{22}$$

$$c \leftarrow \text{soft}(u_2 - d_2, \lambda_2/\mu). \tag{23}$$

To derive the solution to (20a), we make the following substitutions,

$$u = [u_1, u_2]^T, \quad d = [d_1, d_2]^T, \tag{24a}$$

$$\bar{x} = [x, c]^T, \quad M = [I, \quad \Phi], \tag{24b}$$

where $u, d, \bar{x} \in \mathbb{R}^{2N}$. Due to the substitutions, we rewrite (20a) as

$$u \leftarrow \underset{u}{arg\,min} \left\{ \frac{1}{2}\|Hy - HMu\|_2^2 + \frac{\mu}{2}\|u - \bar{x} - d\|_2^2 \right\}. \tag{25}$$

The solution to (25) can be written explicitly as

$$u \leftarrow \left[M^T H^T HM + \mu I_{2N}\right]^{-1} \left[(M^T H^T Hy + \mu(\bar{x} + d)\right], \tag{26}$$

where I_{2N} is the $(2N \times 2N)$ identity matrix. Due to the form (18) of the highpass filter H and the perfect reconstruction property (12) of Φ, we have

$$H^T H = B^T (AA^T)^{-1} B, \tag{27}$$

$$MM^T = 2I. \tag{28}$$

Using the matrix inverse lemma (Tylavsky and Sohie, 1986), (27) and (28), we write

$$\left(M^T H^T HM + \mu I_{2N}\right)^{-1} = \left(M^T B^T (AA^T)^{-1} BM + \mu I_{2N}\right)^{-1} \tag{29}$$

$$= \frac{1}{\mu}\left(I_{2N} - M^T B^T \left[\mu AA^T + 2BB^T\right]^{-1} BM\right). \tag{30}$$

The matrix $\mu AA^T + 2BB^T$ is banded, since the matrices A and B are banded. This is advantageous as the iteration now consists of solving a banded system of equations, rather than a dense system in (29). Combining (30) and (26), we obtain the following procedure for solving (20a)

$$G \leftarrow \left(\mu AA^T + 2BB^T\right) \tag{31a}$$

$$g_1 \leftarrow \frac{1}{\mu} B^T (AA^T)^{-1} By + (x + d_1) \tag{31b}$$

$$g_2 \leftarrow \frac{1}{\mu} \Phi B^T (AA^T)^{-1} By + (c + d_2) \tag{31c}$$

$$u_1 \leftarrow g_1 - B^T G^{-1} B(g_1 + \Phi g_2) \tag{31d}$$

$$u_2 \leftarrow g_2 - \Phi^H B^T G^{-1} B(g_1 + \Phi g_2) \tag{31e}$$

Note that the vector $(1/\mu)B^T(AA^T)^{-1}By$ is used in every iteration. Since the signal y is not updated in each iteration, we need only compute it once before the loop. Combining the routines discussed above, we obtain the DETOKS algorithm.

Algorithm 1 *(DETOKS algorithm).*

inputs
$y \in \mathbb{R}^N, \mu > 0, \lambda_i > 0, \quad i = 0, 1, 2.$
$h \leftarrow (1/\mu)B^T(AA^T)^{-1}By$
repeat:
  $G \leftarrow \left(\mu AA^T + 2BB^T\right)$
  $g_1 \leftarrow h + x + d_1$
  $g_2 \leftarrow \Phi h + (c + d_2)$
  $u_1 \leftarrow g_1 - B^T G^{-1} B(g_1 + \Phi g_2)$
  $u_2 \leftarrow g_2 - \Phi^H B^T G^{-1} B(g_1 + \Phi g_2)$
  $x \leftarrow$ **soft**(**tvd**$(u_1 - d_1, \lambda_1/\mu), \lambda_0/\mu)$
  $c \leftarrow$ **soft**$(u_2 - d_2, \lambda_2/\mu)$
  $d_1 \leftarrow d_1 - (u_1 - x)$
  $d_2 \leftarrow d_2 - (u_2 - c)$
until convergence
$s \leftarrow \Phi c$
$f \leftarrow (y - x - s) - A^{-1}B(y - x - s)$
return x, s, f

After we obtain the estimates for x and c, we calculate the signal components s and f as follows

$$s \leftarrow \Phi c \tag{32}$$

$$f \leftarrow (y - x - s) - A^{-1}B(y - x - s) \tag{33}$$

where we use the highpass filter defined in (15).

Fig. 1 portrays the decomposition of an EEG signal into the signal components f, s and x. The low-frequency component f contains the K-complex, and the oscillatory component s contains the sleep spindles. The non-oscillatory transients are contained in the sparse component x.

3.3. Detection of sleep spindles and K-complexes

The oscillatory component s is used to detect sleep spindles. We bandpass filter s, to remove any non-spindle oscillations using a 4th order Butterworth filter with a passband of 11.5 Hz to 15.5 Hz. We denote this bandpass filtered signal as BPF(s). The TKEO $T(\cdot)$, as defined in (5), is then applied to the signal BPF(s). Using a constant value (c_1) for the threshold, a binary signal $b_{spindle}(t)$, is defined as

$$b_{spindle}(t) = \begin{cases} 1, & T(\text{BPF(s)}) > c_1 \\ 0, & T(\text{BPF(s)}) \le c_1. \end{cases} \tag{34}$$

Any detected spindle of duration less than 0.5 s is rejected. We allow the maximum duration of a detected spindle to be 3 s as in (Warby et al., 2014).

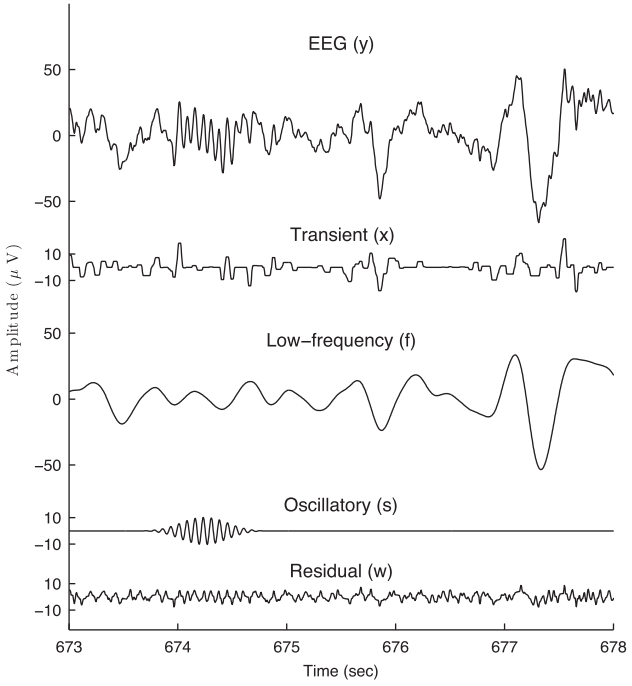

Fig. 1. Decomposition of the raw EEG into the signal components x, f and s using the DETOKS algorithm.

For detecting K-complexes, we apply the TKEO to the low-frequency component f, and define a binary signal $b_{K-complex}(t)$, as in (34), with a constant threshold value (c_2) as

$$b_{K-complex}(t) = \begin{cases} 1, & T(f) > c_2 \\ 0, & T(f) \le c_2. \end{cases} \quad (35)$$

The detected K-complexes of duration less than 0.5 s are rejected.

The DETOKS algorithm uses f and s to detect sleep spindles and K-complexes respectively in sleep EEG. Fig. 2 depicts the proposed detection method. Figs. 3 and 4 show the detection of a sleep spindle and K-complex using DETOKS. The example EEG shown in Fig. 3 is different from the one in Fig. 4, as the expert annotation for K-complexes was not available for the EEG signal in Fig. 3.

4. Examples

We demonstrate the suppression of transients and detection of sleep spindles and K-complexes using DETOKS by applying it to the

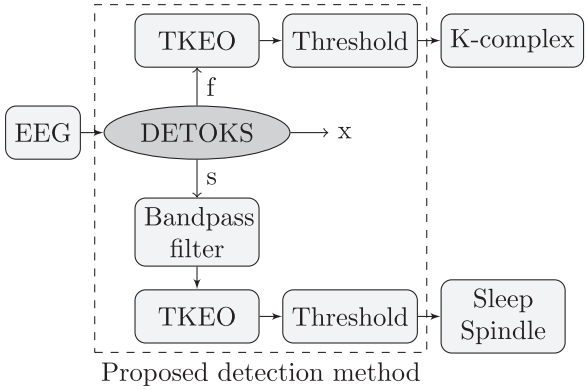

Fig. 2. The detection of sleep spindles and K-complexes using the DETOKS algorithm.

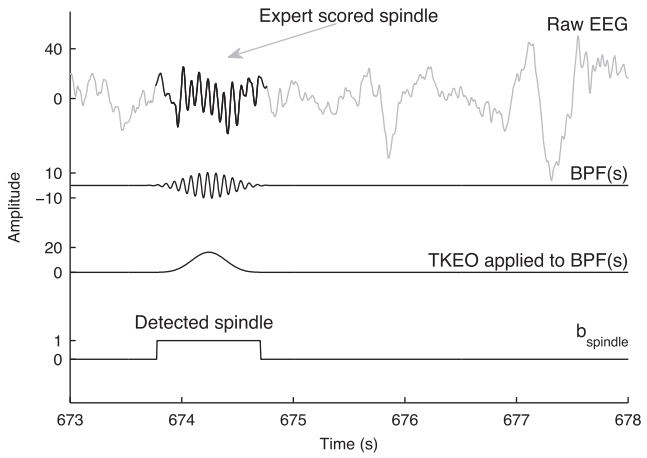

Fig. 3. The detection of a spindle using a Butterworth bandpass filter (BPF) and the TKEO Operator. The value of the constant threshold (c_1) was fixed at 0.03.

C3-A1 channel of an EEG. We compare the performance of DETOKS for sleep spindle detection with the methods proposed by Wendt et al. (2012) and by Martin et al. (2013). We refer the reader to (Warby et al., 2014) for a summary of their detection processes.

Recall that the DETOKS algorithm calls for the specification of the parameters λ_0, λ_1, λ_2 and μ. The parameters λ_0 and λ_1 influence the sparse nature of the component x and its derivative Dx respectively. Similarly, λ_2 controls the time–frequency sparsity of the oscillatory component. For the examples in Fig. 1 and the ones that follow, we use $\lambda_0 = 0.6$, $\lambda_1 = 7$ and $\lambda_2 \in [7.5, 8.5]$. The parameters λ_0, λ_1, and λ_2 were set empirically to ensure that the oscillatory component was free of transients and the detected spindle duration nearly matched the duration of a designated spindle. We use threshold values $c_1 = 0.03$ and $c_2 = 1.0$. Although there is no precise definition for the frequency of K-complexes, they are usually within 0.5–4 Hz (Erdamar et al., 2012; Bremer et al., 1970, Woertz et al.). Therefore, we set the lowpass filter cut-off frequency to 4 Hz.

We use the value $\mu = 0.5$. This value of μ gives the lowest value of the objective function in (17) at the 20th iteration (Fig. 5). Note that μ does not affect the solution to which the DETOKS algorithm converges; it only affects the rate of convergence. Though several parameters must be specified, λ_2 is the only parameter that is varied between [7.5, 8.5] by experimental observation in order to emulate the duration of the detected spindle to that of a designated spindle.

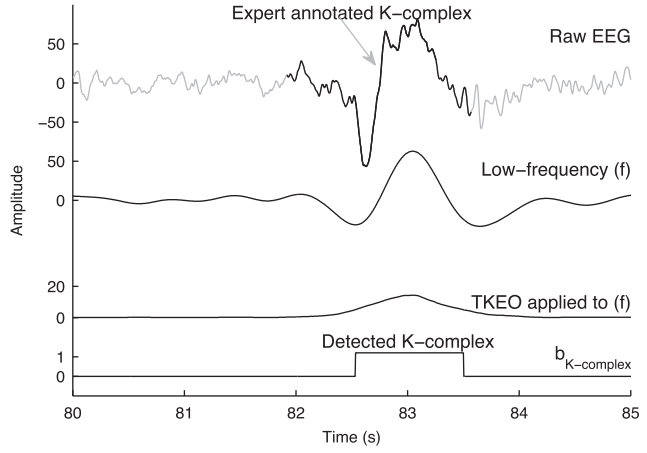

Fig. 4. The detection of K-complex using the TKEO. The value of the constant threshold (c_2) was fixed at 1.

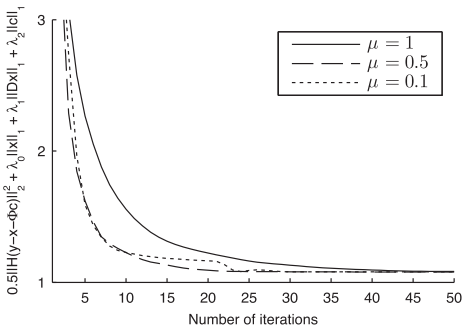

Fig. 5. The convergence of the cost function (17) for different values of μ.

4.1. Sleep spindle detection

We compare the spindle detection of the Wendt, Martin, and the proposed DETOKS method in Fig. 6. Experts have annotated three sleep spindles at 818.1, 820.8 and at 823.9 s. The Martin algorithm detects only two of the spindles, whereas the Wendt algorithm detects only one spindle. On the other hand, all the three spindles are detected by the proposed detection method. The effect of the suppression of transients can be seen in the bandpass filter activity in Fig. 6. The bandpass filter is excited only during spindle activity in the EEG. In contrast, for the Wendt and Martin algorithms, the low amplitude spindle activity is masked by the transients, which excite the bandpass filter. Thus the suppression of transients increases the number of true positives for spindle detection.

As an another example, consider the issue of falsely detected spindles. Fig. 7 illustrates three spindles scored by experts at 131.6, 133.4 and at 138.5 s. However, the Martin and Wendt algorithms each detect an additional spindle, which is not annotated by experts. The transient activity excited the bandpass filters again, to the point that the Wendt and Martin algorithms detect false spindles. On the other hand, DETOKS avoids these false detections. Moreover, the duration of the spindles detected by DETOKS better matches those of the experts.

If the parameters λ_0, λ_1 and λ_2 for the DETOKS algorithm are increased or decreased, then the duration of the spindles detected will also be affected. Thus, one can set the parameters λ_0, λ_1, and λ_2, so that the duration of a detected spindle emulates the duration of a designated spindle.

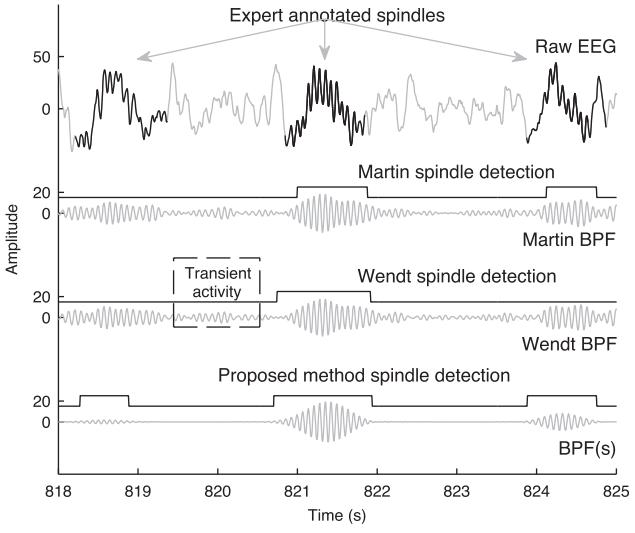

Fig. 6. Comparison of the spindle detection using Wendt, Martin and the proposed detection method.

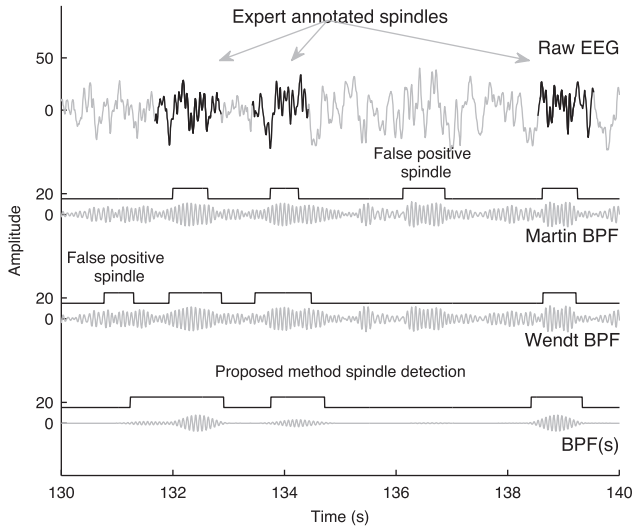

Fig. 7. False detection of spindles by the Wendt and Martin algorithm due to the transient activity in the bandpass filtered data.

4.2. K-complex detection

Conventional methods for K-complex detection apply a lowpass filter directly to the EEG then use the TKEO. However, this yields a large number of false positives as seen in Fig. 8. There is only one true positive K-complex at 254.4 s and four false positives. Removal of these false positives requires additional processing stages rather than simply using the TKEO on the lowpass filtered EEG (Erdamar et al., 2012). The transients in the EEG excite the lowpass filter, which are then mis-identified as K-complexes after the TKEO stage. Moreover, increasing the threshold for TKEO will not only result in low true positive values, but the duration of the detected K-complexes will also be shorter compared to the expert annotation. In contrast, the component x obtained using the DETOKS algorithm captures the transient activity, thereby reducing the number of false positives while accurately detecting the designated K-complexes.

Fig. 9 compares the K-complexes detected using the proposed method and the method by Devuyst et al. (2010). Specifically, we

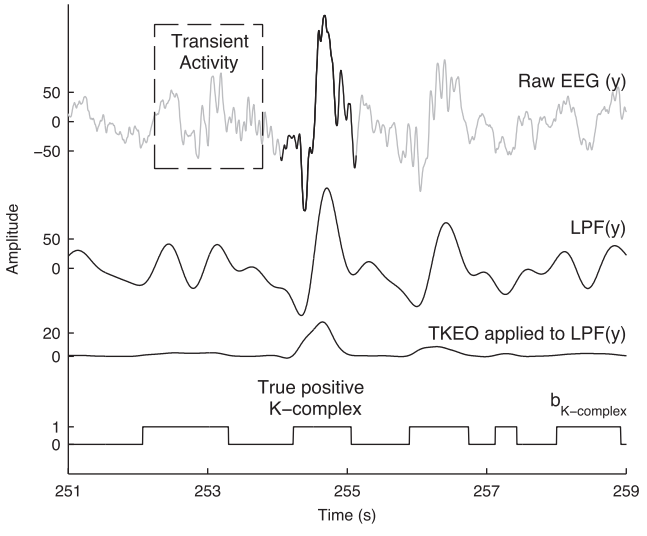

Fig. 8. Detecting K-complexes with a 4th order Butterworth lowpass filter LPF(·) and the TKEO. There are four false positive K-complexes and only one true positive.

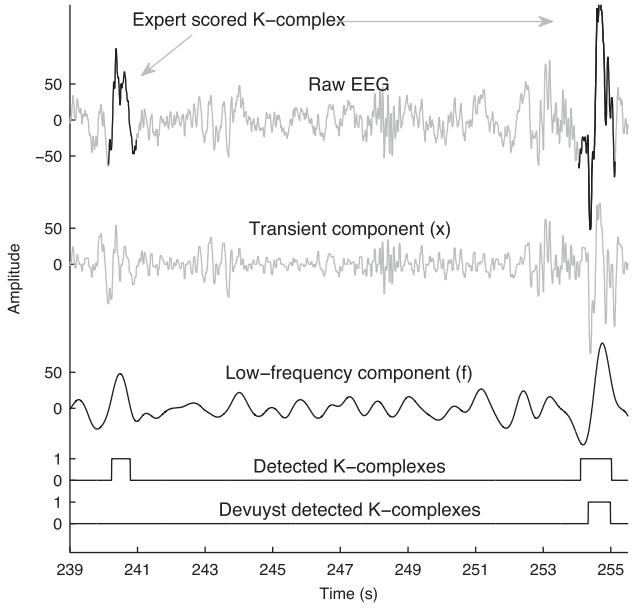

Fig. 9. Comparison of the K-complex detection by Devuyst et al. and the proposed simultaneous detection method. The transients in the EEG are captured in the component x.

compare the annotations provided by Devuyst et al. online[2] for their method, and the K-complex detection by DETOKS. The experts have annotated two K-complexes – at 240 and at 254 s. The component f obtained by the proposed method is also shown. It can be seen that the Devuyst algorithm (Devuyst et al., 2010) detects only the K-complex at 255 s. Moreover, the duration of the detected K-complex is less than that indicated by the expert. On the other hand, DETOKS detects both K-complexes which better match the expert detection.

5. Evaluation of DETOKS

We assess the performance of DETOKS by applying it to an online EEG database. We use two publicly available databases[3] – one for spindle detection and one for K-complex detection. The databases[4] are made available online by Devuyst et al. (2011). For both, spindle and K-complex detection, we use the central channel C3-A1 of the EEG. We use these databases for the evaluation study because they are readily available online and provide expert annotations for the scoring of sleep spindles and K-complexes.

5.1. Database

As per (Devuyst et al., 2011), the EEG database for sleep spindle detection was acquired in a sleep laboratory of a Belgium hospital using a digital 32-channel polygraph (BrainnetTM System of MEDATEC, Brussels, Belgium). The patients possessed different pathologies (dysomnia, restless legs syndrome, insomnia, apnoea/hypopnoea syndrome) (Devuyst et al., 2011). Three EEG channels (CZ-A1 or C3-A1, FP1-A1, and O1-A1), two EOG channels and one submental EMG channel were recorded. A 30-min segment of the central EEG channel was extracted from each whole-night recording for sleep spindle scoring. These excerpts were given to two experts who independently scored spindles. Out of the 8 excerpts, we conduct the study using the 5 excerpts that were annotated by both experts.

The EEG database for K-complex detection was also acquired in a sleep laboratory of a Belgium hospital using a digital 32-channel polygraph (BrainnetTM System of MEDATEC, Brussels, Belgium) (Devuyst et al., 2010). As in the case of the sleep spindles, a 30-min segment from each whole-night recording was independently given to two experts for scoring of K-complexes according to the manual (Berry et al., 2013) and the recommendations in (Devuyst et al., 2010). For this study, we use the 5 excerpts that were scored by both experts.

Table 1
K-complex detection performance evaluation.

	Devuyst et al.	DETOKS
F_1 score	0.51	0.57
Recall	0.40	0.61
Precision	0.74	0.56

5.2. Existing detection methods

For sleep-spindle detection, we compare DETOKS to the existing algorithms by Wendt et al. (S1) (Wendt et al., 2012), Martin et al. (S2) (Martin et al., 2013), Wamsley et al. (S3) (Wamsley et al., 2012), Bòdizs et al. (S4) (Bódizs et al., 2009), Mölle et al. (S5) (Gais et al., 2002), and Devuyst et al. (S6) (Devuyst et al., 2011). A summary of these algorithms is provided in (Warby et al., 2014; Devuyst et al., 2011). We reject any spindles detected by S1–S6 of less than 0.5 s in duration. For K-complex detection we compare DETOKS to the annotations provided by Devuyst et al. for their detection method (Devuyst et al., 2010).

5.3. Measure of performance

We use the detection by experts, for the sleep spindles and the K-complexes, as the gold standard. A sample point of the EEG is recorded as a sleep spindle or a K-complex if it was scored as such by either expert. This is the by-sample analysis of a detector (Warby et al., 2014) using a 'union' rule of the expert detection (Devuyst et al., 2011). We create a contingency table, for sleep spindles and K-complexes, to calculate the values of true positive (TP), false positive (FP), true negative (TN) and false negative (FN). These values are then used to calculate the recall and precision values for the detector. We use F_1 scores to evaluate the detectors. The F_1 score ranges from 0 to 1, with 1 denoting the perfect detector. Using the contingency table, the statistical measures of Cohen's κ (Cohen, 1960) and Matthews Correlation Coefficient (MCC) (Matthews, 1975) can also be calculated.

5.4. Results

The C3-A1 channel of the EEG was processed using the proposed DETOKS algorithm and the estimates of the components s and f were then used for sleep spindle and K-complex detection respectively. We used the same parameters for $\lambda_0, \lambda_1, \lambda_2$ and the threshold values c_1 and c_2 as in Section 4. We used the STFT parameters given in Section 2.3.

Fig. 10 displays the F_1 scores for sleep spindle detection, recall, and precision values for the algorithms in Section 5.2 and DETOKS. Table 1 lists the F_1 scores for K-complex detection for the Devuyst algorithm (Devuyst et al., 2010) and DETOKS. The recall and precision values are also listed.

Further statistical measures of performance are listed in the Appendix. The proposed DETOKS method takes about 4 min to run 20 iterations on approximately 8 h of EEG at sampling frequency 100 Hz.

[2] http://www.tcts.fpms.ac.be/ devuyst/Databases/DatabaseKcomplexes/.
[3] http://www.tcts.fpms.ac.be/ devuyst/#Databases.
[4] University of MONS – TCTS Laboratory (S. Devuyst, T. Dutoit) and Universite Libre de Bruxelles – CHU de Charleroi Sleep Laboratory (M. Kerkhofs).

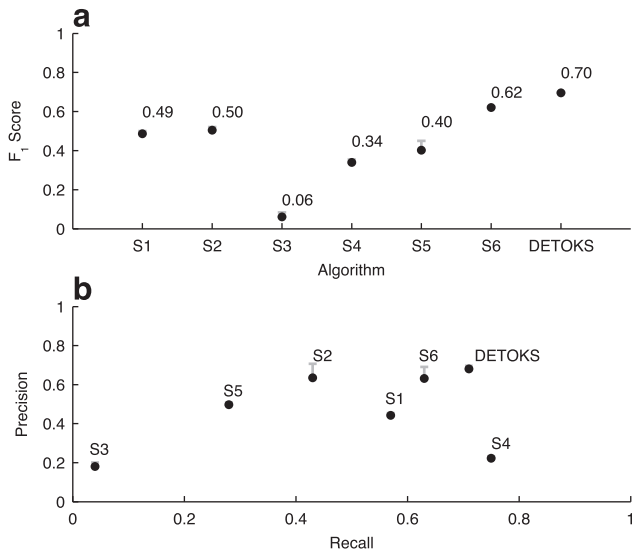

Fig. 10. Results of the evaluation study in Section 5. (a) Comparison of the F_1 scores of the spindle detection algorithms. (b) Recall and Precision values for the algorithms S1–S6 and the proposed DETOKS method. The error bars represent standard error of the mean.

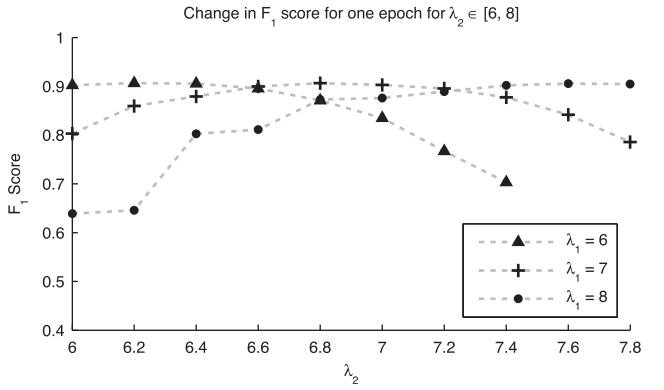

Fig. 11. Change in the F_1 score of an epoch on changing the parameters λ_1 and λ_2 in (17). λ_0 is fixed at 0.6.

5.5. Discussions

The proposed DETOKS method achieves high F_1 scores for spindle detection due to the suppression of transients. As seen in Appendix A, the values of κ and MCC were similar to the F_1 scores obtained. The TP values are comparatively higher than those of algorithms S1–S6. The number of false positives are also reduced. The reduction in FP values and an increase in TP values, result in the F_1 score of the proposed detection method for sleep spindles averaging 0.7 ± 0.03 over the five excerpts. Note that an extensive study on sleep spindle detection by automated detectors (Warby et al., 2014) showed that the F_1 score of 24 individual experts averaged 0.69 ± 0.06 on their crowd-sourcing generated spindle gold standard. The proposed DETOKS method achieves the average F_1 score of an expert consistently, thus making it a reliable spindle detector.

A balanced detector shows high recall and precision values. Fig. 10 shows that DETOKS is the most balanced among the 6 algorithms S1–S6 for spindle detection. The recall and precision values for DETOKS averaged 0.71 ± 0.01 and 0.68 ± 0.03 respectively. The algorithm by Bódizs et al. (2009) has a higher recall than the DETOKS but low precision, indicating the detection of a large number of false positives in contrast to DETOKS. The proposed DETOKS method is not only reliable but also a balanced spindle detector.

For the detection of K-complexes, the proposed method obtained an average F_1 score of 0.57 ± 0.019 over the 5 excerpts. The performance of DETOKS for K-complex detection was also balanced compared to the Devuyst algorithm (Devuyst et al., 2010). It can be seen in Table 1, that the proposed detection method has better recall and precision values compared to the Devuyst algorithm. Note that the recall, precision, and F_1 scores for the Devuyst method were calculated based on the TP, FP, TN, and FN values provided in (Devuyst et al., 2010).

The algorithm by Devuyst et al. employs K-complex detection using a training dataset (Devuyst et al., 2010). It tunes the detection process, based on visually identified K-complexes. In contrast, the proposed detection method needs no training data-set. Moreover, for different databases, based on the sampling frequency, the only parameters that need to be tuned are the regularization parameters λ_0, λ_1 and λ_2. The other parameters, for example the STFT window length, are based on the definition of sleep spindles and hence need no tuning. Fig. 11 shows that the F_1 score for sleep spindle detection for one EEG epoch is affected marginally when the parameters λ_1 and λ_2 are changed in small increments, with λ_0 fixed. Similar change is observed when λ_0 is varied in addition to λ_1 and λ_2.

6. Conclusion

This paper proposes an EEG signal model comprising of (1) a transient component, (2) a low-frequency component, and (3) an oscillatory component with sparse time–frequency representation. We propose a convex optimization algorithm for the detection of K-complexes and sleep spindles (DETOKS), which estimates the three components in the signal model. The proposed DETOKS method utilizes the Teager–Kaiser Energy Operator (TKEO) as a means to obtain the envelope of the bandpass filtered oscillatory component and the low-frequency component. The envelopes are then used for the detection of sleep spindles and K-complexes.

An assessment of the proposed DETOKS method yields F_1 scores of average 0.70 ± 0.03 for sleep spindle detection and 0.57 ± 0.019 for K-complex detection. The proposed signal model and the DETOKS algorithm give better results for the detection of both sleep spindles and K-complexes, compared to existing algorithms specifically aimed at one or the other. The average F_1 score of the proposed detector is about the same as the F_1 score attained by individual experts annotating crowd-sourced spindle data (Warby et al., 2014). Comparable run-times and better detection results than traditional spindle and K-complex detection algorithms suggest that the proposed DETOKS method is practical for the detection of sleep spindles and K-complexes.

Appendix A. K-complex detection

	Excerpt 1		Excerpt 2		Excerpt 3		Excerpt 4		Excerpt 5	
	Devuyst	DETOKS	Devuyst	DETOKS	Devuyst	DETOKS	Devuyst	DETOKS	Devuyst	DETOKS
TP	2646	4777	4800	7824	1676	1973	6672	10404	4840	7140
TN	349221	341758	348236	343917	355906	355150	335746	331796	347611	345900
FP	627	8089	1337	5655	889	1644	2674	6623	1869	3580
FN	7506	5375	5627	2603	1529	1232	14908	11176	5680	3380
Recall	0.261	0.471	0.460	0.750	0.523	0.616	0.309	0.482	0.460	0.679
Precision	0.808	0.371	0.782	0.580	0.653	0.545	0.714	0.611	0.721	0.666
F1 Score	**0.394**	**0.415**	**0.580**	**0.655**	**0.581**	**0.578**	**0.431**	**0.539**	**0.562**	**0.672**
Specificity	0.998	0.977	0.996	0.984	0.998	0.995	0.992	0.980	0.995	0.990
NPV	0.979	0.985	0.984	0.992	0.996	0.997	0.957	0.967	0.984	0.990
Accuracy	0.977	0.963	0.981	0.977	0.993	0.992	0.951	0.951	0.979	0.981
Kappa	**0.386**	**0.396**	**0.570**	**0.643**	**0.578**	**0.574**	**0.410**	**0.513**	**0.552**	**0.652**
MCC	**0.451**	**0.399**	**0.591**	**0.649**	**0.581**	**0.575**	**0.450**	**0.517**	**0.566**	**0.661**

Fig. 12. Performance and comparison of the proposed method forK-complex detection with Devuyst et al.

Appendix B. Sleep spindle detection

Excerpt 1	Wendt	Martin	Wamsley	Bodizs	Moelle	Devuyst	DETOKS
TP	8357	4121	2374	9550	4991	9692	9354
TN	156774	164771	166242	137540	164911	159737	162632
FP	9751	1754	283	28985	1614	6788	3892
FN	5118	9354	11101	3925	8484	3783	4121
Recall	0.620	0.306	0.176	0.709	0.370	0.719	0.694
Precision	0.462	0.701	0.893	0.248	0.756	0.588	0.706
F1 Score	**0.529**	**0.426**	**0.294**	**0.367**	**0.497**	**0.647**	**0.700**
Specificity	0.941	0.989	0.998	0.826	0.990	0.959	0.977
NPV	0.968	0.946	0.937	0.972	0.951	0.977	0.975
Accuracy	0.917	0.938	0.937	0.817	0.944	0.941	0.955
Kappa	**0.485**	**0.399**	**0.276**	**0.288**	**0.471**	**0.615**	**0.676**
MCC	**0.491**	**0.437**	**0.381**	**0.343**	**0.505**	**0.619**	**0.676**

Excerpt 2	Wendt	Martin	Wamsley	Bodizs	Moelle	Devuyst	DETOKS
TP	9881	7954	0	11045	7006	9862	10307
TN	320771	339807	344818	268002	340517	336140	339091
FP	24754	5718	707	77523	5008	9385	6433
FN	4594	6521	14475	3430	7469	4613	4168
Recall	0.683	0.549	0.000	0.763	0.484	0.681	0.71
Precision	0.285	0.582	0.000	0.125	0.583	0.512	0.62
F1 Score	**0.402**	**0.565**	**0.000**	**0.214**	**0.529**	**0.585**	**0.67**
Specificity	0.928	0.983	0.998	0.776	0.986	0.973	0.98
NPV	0.986	0.981	0.960	0.987	0.979	0.986	0.99
Accuracy	0.918	0.966	0.958	0.775	0.965	0.961	0.97
Kappa	**0.366**	**0.548**	**-0.004**	**0.156**	**0.511**	**0.565**	**0.65**
MCC	**0.407**	**0.548**	**-0.009**	**0.246**	**0.514**	**0.571**	**0.65**

Excerpt 3	Wendt	Martin	Wamsley	Bodizs	Moelle	Devuyst	DETOKS
TP	1005	680	12	0.00	0	1400	1707
TN	86050	87234	86741	0.00	87717	86882	86772
FP	1667	483	976	0.00	0	835	944
FN	1278	1603	2271	0.00	2283	883	576
Recall	0.440	0.298	0.005	0.00	0.000	0.613	0.748
Precision	0.376	0.585	0.012	0.00	0.000	0.626	0.644
F1 Score	**0.406**	**0.395**	**0.007**	0.00	**0.000**	**0.620**	**0.692**
Specificity	0.981	0.994	0.989	0.00	1.000	0.990	0.989
NPV	0.985	0.982	0.974	0.00	0.975	0.990	0.993
Accuracy	0.967	0.977	0.964	0.00	0.975	0.981	0.983
Kappa	**0.389**	**0.384**	**-0.008**	0.00	**0.000**	**0.610**	**0.683**
MCC	**0.390**	**0.407**	**-0.009**	0.00	**0.000**	**0.610**	**0.685**

Excerpt 5	Wendt	Martin	Wamsley	Bodizs	Moelle	Devuyst	DETOKS
TP	10461	9672	0	14779	0	10332	14164
TN	330466	333514	337779	295704	340039	335566	333646
FP	9573	6525	2260	44335	0	4473	6392
FN	9500	10289	19961	5182	19961	9629	5797
Recall	0.524	0.485	0.000	0.740	0.000	0.518	0.710
Precision	0.522	0.597	0.000	0.250	0.000	0.698	0.689
F1 Score	**0.523**	**0.535**	**0.000**	**0.374**	**0.000**	**0.594**	**0.699**
Specificity	0.972	0.981	0.993	0.870	1.000	0.987	0.981
NPV	0.972	0.970	0.944	0.983	0.945	0.972	0.983
Accuracy	0.947	0.953	0.938	0.862	0.945	0.961	0.966
Kappa	**0.495**	**0.511**	**-0.011**	**0.317**	**0.000**	**0.574**	**0.681**
MCC	**0.495**	**0.514**	**-0.019**	**0.377**	**0.000**	**0.581**	**0.681**

Excerpt 6	Wendt	Martin	Wamsley	Bodizs	Moelle	Devuyst	DETOKS
TP	12810	11724	0	17988	11928	13381	15435
TN	327975	332715	336704	288379	331078	332761	332467
FP	9588	4848	859	49184	6485	4802	5095
FN	9627	10713	22437	4449	10509	9056	7002
Recall	0.571	0.523	0.000	0.802	0.532	0.596	0.688
Precision	0.572	0.707	0.000	0.268	0.648	0.736	0.752
F1 Score	**0.571**	**0.601**	**0.000**	**0.401**	**0.584**	**0.659**	**0.718**
Specificity	0.972	0.986	0.997	0.854	0.981	0.986	0.985
NPV	0.971	0.969	0.938	0.985	0.969	0.974	0.979
Accuracy	0.947	0.957	0.935	0.851	0.953	0.962	0.966
Kappa	**0.543**	**0.579**	**-0.005**	**0.340**	**0.559**	**0.639**	**0.701**
MCC	**0.543**	**0.586**	**-0.013**	**0.407**	**0.562**	**0.643**	**0.701**

Fig. 13. Performance of the proposed DETOKS method for spindle detection and comparison with other widely used algorithms.

References

Acir N, Güzeli C. Automatic recognition of sleep spindles in EEG via radial basis support vector machine based on a modified feature selection algorithm. Neural Comput Appl 2005];14(1):56–65, http://dx.doi.org/10.1007/s00521-004-0442-z, ISSN 0941-0643.

Afonso M, Bioucas-Dias J, Figueiredo M. Fast image recovery using variable splitting and constrained optimization. IEEE Trans Image Process 2010];19:2345–56, http://dx.doi.org/10.1109/TIP.2010.2047910, ISSN 1941-0042.

Bódizs R, Körmendi J, Rigó P, Lázár AS. The individual adjustment method of sleep spindle analysis: methodological improvements and roots in the fingerprint paradigm. J Neurosci Methods 2009];178(1):205–13, http://dx.doi.org/10.1016/j.jneumeth.2008.11.006, ISSN 0165-0270.

Berry R, Brooks R, Gamaldo C, Harding S, Lloyd R, Marcus C, et al. The AASM manual for the scoring of sleep and associated events: rules, terminology and technical specifications; 2013].

Boyd S, Parikh N, Chu E, Eckstein J. Distributed optimization and statistical learning via the alternating direction method of multipliers. Found Trends Mach Learn 2010];3(1):1–122, http://dx.doi.org/10.1561/2200000016, ISSN 1935-8237.

Bremer G, Smith JR, Karacan I. Automatic detection of the K-complex in sleep electroencephalograms. IEEE Trans Bio-med Eng 1970];17:314–23, http://dx.doi.org/10.1109/TBME.1970.4502759, ISSN 0018-9294.

Camilleri TA, Camilleri KP, Fabri SG. Automatic detection of spindles and K-complexes in sleep EEG using switching multiple models. Biomed Signal Process Control 2014];10:117–27, http://dx.doi.org/10.1016/j.bspc.2014.01.010, ISSN 17468094.

Chambolle A, Pock T. A first-order primal-dual algorithm for convex problems with applications to imaging. J Math Imaging Vis 2011];40(1):120–45, http://dx.doi.org/10.1007/s10851-010-0251-1, ISSN 09249907.

Chen S, Donoho DL, Saunders MA. Atomic decomposition by basis pursuit. SIAM J Sci Comput 1998];43(1):129–59, http://dx.doi.org/10.1137/S1064827596304010.

Cohen J. A coefficient of agreement for nominal scales. Educ Psychol Meas 1960];20(1):37–46, http://dx.doi.org/10.1177/001316446002000104.

Combettes PL, Pesquet J-C. Proximal thresholding algorithm for minimization over orthonormal bases. SIAM J Optim 2007];18(4):1351–76, http://dx.doi.org/10.1137/060669498, ISSN 1052-6234.

Combettes PL, Pesquet J-C. Proximal splitting methods in signal processing. In: Bauschke HH, Others, editors. Fixed-point algorithms for inverse problems in science and engineering. Springer-Verlag; 2011]. p. 185–212.

Condat L. A direct algorithm for 1-D total variation denoising. IEEE Signal Process Lett 2013];20(11):1054–7, http://dx.doi.org/10.1109/LSP.2013.2278339, ISSN 1070-9908.

Costa J, Ortigueira M, Batista A, Paiva L. An automatic sleep spindle detector based on WT, STFT and WMSD. World Academy of Science, Engineering and Technology; 2012]. p. 1833–6.

Devuyst S, Dutoit T, Didier J, Meers F, Stanus E, Stenuit P, et al. Automatic sleep spindle detection in patients with sleep disorders. In: Proceedings of the IEEE International Conference of Engineering in Medicine and Biology (EMBC); 2006]. p. 3883–6, http://dx.doi.org/10.1109/IEMBS.2006.259298, ISSN 1557-170X.

Devuyst S, Dutoit T, Stenuit P, Kerkhofs M. Automatic K-complexes detection in sleep EEG recordings using likelihood thresholds. In: Proceedings of the IEEE International Conference of Engineering in Medicine and Biology (EMBC); 2010]., http://dx.doi.org/10.1109/IEMBS.2010.5626447, ISBN 9781424441235 ISSN 1557-170X 4658-4661.

Devuyst S, Dutoit T, Stenuit P, Kerkhofs M. Automatic sleep spindles detection – overview and development of a standard proposal assessment method. In: Proceedings of the IEEE International Conference of Engineering in Medicine and Biology (EMBC); 2011]. p. 1713–6, http://dx.doi.org/10.1109/IEMBS.2011.6090491, ISSN 1557-170X.

Donoho DL. De-noising by soft-thresholding. IEEE Trans Inf Theory 1995];41:613–27, http://dx.doi.org/10.1109/18.382009, ISSN 00189448.

Durka P, Blinowska K. Matching pursuit parametrization of sleep spindles. Eng Med Biol 1996];3:1011–2, http://dx.doi.org/10.1109/IEMBS.1996.652685.

Durka P, Ircha D, Blinowska K. Stochastic time–frequency dictionaries for matching pursuit. IEEE Trans Signal Process 2001];49(3):507–10, http://dx.doi.org/10.1109/78.905866, ISSN 1053587X.

Erdamar A, Duman F, Yetkin S. A wavelet and Teager energy operator based method for automatic detection of K-complex in sleep EEG. Expert Syst Appl 2012];39(1):1284–90, http://dx.doi.org/10.1016/j.eswa.2011.07.138, ISSN 09574174.

Ferrarelli F, Huber R, Peterson MJ, Massimini M, Murphy M, Riedner BA, et al. Reduced sleep spindle activity in schizophrenia patients. Am J Psychiatry 2007];164(3):483–92, http://dx.doi.org/10.1176/appi.ajp.164.3.483, ISSN 0002-953X.

Fogel SM, Smith CT. The function of the sleep spindle: a physiological index of intelligence and a mechanism for sleep-dependent memory consolidation. Neurosci Biobehav Rev 2011];35(5):1154–65, http://dx.doi.org/10.1016/j.neubiorev.2010.12.003, ISSN 1873-7528.

Gabay D. Applications of the method of multipliers to variational inequalities. In: Augmented Lagrangian methods: applications to the numerical solution of boundary-value problems. Elsevier; 1983]. p. 299–331.

Gais S, Mölle M, Helms K, Born J. Learning-dependent increases in sleep spindle density. J Neurosci: Off J Soc Neurosci 2002];22(15):6830–4, ISSN 1529-2401, doi:20026697.

Gorur D, Halici U, Aydin H. Sleep spindles detection using short time Fourier transform and neural networks. International Joint Conference on Neural Networks (IJCNN) 2002]:1631–6.

Jaleel A, Ahmed B, Tafreshi R, Boivin DB, Streletz L, Haddad N. Improved spindle detection through intuitive pre-processing of electroencephalogram. J Neurosci Methods 2014];233:1–12, http://dx.doi.org/10.1016/j.jneumeth.2014.05.009, ISSN 1872-678X.

Limoges E, Mottron L, Bolduc C, Berthiaume C, Godbout R. Atypical sleep architecture and the autism phenotype. Brain: J Neurol 2005];128(Pt 5):1049–61, http://dx.doi.org/10.1093/brain/awh425, ISSN 1460-2156.

Mallat S. Sparse representations. In: A wavelet tour of signal processing: the sparse way. Academic Press; 2009]. p. 1–31, Chapter 1, ISBN 978-0-12-374370-1, doi:10.1016/B978-0-12-374370-1.00005-7.

Martin N, Lafortune M, Godbout J, Barakat M, Robillard R, Poirier G, et al. Topography of age-related changes in sleep spindles. Neurobiol Aging 2013];34(2):468–76, http://dx.doi.org/10.1016/j.neurobiolaging.2012.05.020, ISSN 1558-1497.

Matthews BW. Comparison of the predicted and observed secondary structure of T4 phage lysozyme. Biochim Biophys Acta (BBA) – Protein Struct 1975];405(2):442–51, http://dx.doi.org/10.1016/0005-2795(75)90109-9.

Motamedi-Fakhr S, Moshrefi-Torbati M, Hill M, Hill CM, White PR. Signal processing techniques applied to human sleep EEG signals: a review. Biomed Signal Process Control 2014];10:21–33, http://dx.doi.org/10.1016/j.bspc.2013.12.003, ISSN 17468094.

Parekh A, Selesnick IW, Rapoport DM, Ayappa I. Sleep spindle detection using time–frequency sparsity. In: Proceedings of the IEEE Signal Processing in Medicine and Biology Symposium (SPMB); 2014]., http://dx.doi.org/10.1109/SPMB.2014.7002965.

Petit D, Gagnon JF, Fantini ML, Ferini-Strambi L, Montplaisir J. Sleep and quantitative EEG in neurodegenerative disorders. J Psychosom Res 2004]., http://dx.doi.org/10.1016/j.jpsychores.2004.02.001.

Richard C, Lengelle R. Joint time and time–frequency optimal detection of K-complexes in sleep EEG. Comput Biomed Res: Int J 1998];31:209–29, ISSN 0010-4809, doi: S0010480998914768 [pii].

Rinaldo A. Properties and refinements of the fused lasso. Ann Stat 2009];37(5B):2922–52, http://dx.doi.org/10.1214/08-AOS665, ISSN 0090-5364.

Rudin LI, Osher S, Fatemi E. Nonlinear total variation based noise removal algorithms. Phys D: Nonlinear Phenom 1992];60:259–68, http://dx.doi.org/10.1016/0167-2789(92)90242-F, ISSN 01672789.

Selesnick IW, Graber HL, Pfeil DS, Barbour RL. Simultaneous low-pass filtering and total variation denoising. IEEE Trans Signal Process 2014];62(5):1109–24, http://dx.doi.org/10.1109/TSP.2014.2298836, ISSN NA.

Selesnick IW. Resonance-based signal decomposition: a new sparsity-enabled signal analysis method. Signal Process 2011];91(12):2793–809, http://dx.doi.org/10.1016/j.sigpro.2010.10.018, ISSN 01651684.

Selesnick IW. Short-time Fourier transform and speech denoising; 2015] http://cnx.org/content/m32294/

Silber MH, Ancoli-Israel S, Bonnet MH, Chokroverty S, Grigg-Damberger MM, Hirshkowitz M, et al. The visual scoring of sleep in adults. J Clin Sleep Med: JCSM: Off Publ Am Acad Sleep Med 2007];3(2):121–31, ISSN 1550-9389.

Stepnowsky C, Levendowski D, Popovic D, Ayappa I, Rapoport DM. Scoring accuracy of automated sleep staging from a bipolar electroocular recording compared to manual scoring by multiple raters. Sleep Med 2013];14(11):1199–207, http://dx.doi.org/10.1016/j.sleep.2013.04.022, ISSN 1878-5506.

Strungaru C, Popescu MS. Neural network for sleep EEG K-complex detection. Biomed Tech[[nl]]Biomed Eng 1998];43(Suppl. 3):113–6, http://dx.doi.org/10.1515/bmte.1998.43.s3.113, ISSN 0013-5585.

Tibshirani R, Saunders M, Rosset S, Zhu J, Knight K. Sparsity and smoothness via the fused lasso. J R Stat Soc Ser B: Stat Methodol 2005;67:91–108, http://dx.doi.org/10.1111/j.1467-9868.2005.00490.x, ISSN 13697412.

Tylavsky D, Sohie G. Generalization of the matrix inversion lemma. In: Proceedings of the IEEE; 1986]. p. 1050–2, http://dx.doi.org/10.1109/PROC.1986.13587, ISSN 0018-9219.

Wamsley E, Tucker M, Shinn A. Reduced sleep spindles and spindle coherence in schizophrenia: mechanisms of impaired memory consolidation? Biol Psychiatry 2012];71(2):154–61, http://dx.doi.org/10.1016/j.biopsych.2011.08.008, Reduced.

Warby SC, Wendt SL, Welinder P, Munk EGS, Carrillo O, Sorensen HBD, et al. Sleep-spindle detection: crowdsourcing and evaluating performance of experts, non-experts and automated methods. Nat Methods 2014];11(4):385–92, http://dx.doi.org/10.1038/nmeth.2855, ISSN 1548-7105.

Wendt SL, Christensen JE, Kempfner J, Leonthin HL, Jennum P, Sorensen HBD. Validation of a novel automatic sleep spindle detector with high performance during sleep in middle aged subjects. In: Proceedings of the IEEE International Conference of Engineering in Medicine and Biology (EMBC); 2012]. p. 4250–3, http://dx.doi.org/10.1109/EMBC.2012.6346905, ISSN 1557-170X.

Woertz M, Miazhynskaia T, Anderer P, Dorffner G. Automatic K-complex detection: comparison of two different approaches, Abstracts of the ESRS. JSR 2004;13(1).